Chinese Journal of Aeronautics, 2013,26(1): 122–129

Chinese Society of Aeronautics and Astronautics
& Beihang University

Chinese Journal of Aeronautics

cja@buaa.edu.cn
www.sciencedirect.com

Research on failure criterion of composite based on unified macro- and micro-mechanical model

Sun Zhigang *, Zhao Long, Chen Lei, Song Yingdong

College of Energy and Power Engineering and State Key Laboratory of Mechanics and Control of Mechanical Structures, Nanjing University of Aeronautics and Astronautics, Nanjing 210016, China

Received 14 October 2011; revised 21 November 2011; accepted 12 December 2011
Available online 16 January 2013

KEYWORDS

Composite;
Finite-volume direct averaging micromechanics;
Mechanics failure model;
Multi-scale finite element;
Unified macro and micro

Abstract A new unified macro- and micro-mechanics failure analysis method for composite structures was developed in order to take the effects of composite micro structure into consideration. In this method, the macro stress distribution of composite structure was calculated by commercial finite element analysis software. According to the macro stress distribution, the damage point was searched and the micro-stress distribution was calculated by reformulated finite-volume direct averaging micromechanics (FVDAM), which was a multi-scale finite element method for composite. The micro structure failure modes were estimated with the failure strength of constituents. A unidirectional composite plate with a circular hole in the center under two kinds of loads was analyzed with the traditional macro-mechanical failure analysis method and the unified macro- and micro-mechanics failure analysis method. The results obtained by the two methods are consistent, which show this new method's accuracy and efficiency.

1. Introduction

Composite materials are utilized more and more widely in many engineering structures because of high strength and low density. In future, they will be used vastly in all kinds of aerospace, automotive, marine vehicles structures, etc. For engineering applications, it is necessary to establish a strength model in order to predict the failure of material.

Nowadays, macroscopic theories of strength are broadly employed (e.g., maximum stress criteria, maximum strain criteria and cross correlation criteria).[1] In the macro theory of strength, composite is assumed to be homogeneous and damage criteria is adopted as macro-phenomenon in material tests. Nevertheless, composite is composed of matrix and fiber which is transversely isotropic, and the damage forms (e.g. fiber fracture, matrix cracking and interface failure) are closely related to the micro-characters; therefore, it is quite necessary to research failure process and strength of composite with micro-mechanics methods.

In 1989, Aboudi proposed a unified macro- and micro-mechanics failure model with method of cells.[2] Then Paley and Aboudi developed generalized method of cells (GMC),[3] and GMC reformulated by Pindera and Bednarcyk[4] for enhanced efficiency was used to analyze three-dimensional stress distribution in unidirectional composites. Because GMC employs a first-order representation of the displacement field in each sub-volume of the repeating unit cell, the accuracy with which local stress and strain fields are captured (although acceptable in many applications) is not good. It requires the

* Corresponding author. Tel.: +86 25 84892206 2506.
E-mail address: szg_mail@nuaa.edu.cn (Z. Sun).

Peer review under responsibility of Editorial Committe of CJA.

ELSEVIER Production and hosting by Elsevier

1000-9361 © 2013 CSAA & BUAA. Production and hosting by Elsevier Ltd. Open access under CC BY-NC-ND license.
http://dx.doi.org/10.1016/j.cja.2012.12.015

incorporation of additional assumptions and modifications into the model's framework in order to analysis the damage of composite at the load level, for instance, fiber breakage and fiber/matrix interface deboning. The higher-order displacement representation was applied to the GMC to provide the necessary coupling between the local normal and shear deformation fields and the macroscopically applied average strains. This new method is called high-fidelity generalized method of cells (HFGMC).[5] Pindera[6–8] and Sun et al.[9–11], improved the theory and advanced the efficiency of HFGMC. Bansal and Pindera[6,7] named their model as finite-volume direct averaging micromechanics (FVDAM). In their models, surface-averaged quantities which replace the coefficients of the displacement are the primary variables, and the research works about FVDAM are summarized in detail in Ref.[7] FVDAM is a kind of micro-mechanics method which can be used to describe the constitute model of composite. Based on the supposition of periodicity in composite microstructure, a unit cell representative of the material microstructure is divided into a number of sub-volumes, and in FVDAM, the displacement expression is supposed to be an interpolation function of the displacement of the center in a sub-volume. According to average displacement and stress continuity condition, the elastic mechanics equations are solved, and the stress and strain distributing are obtained in the unit cell. The relationship between global stress and global strain can be obtained by homogenization and the constitute model for composite is established.

The research of the constitutive model mentioned above does not consider faint of the composites. This thesis develops an analysis method for the damage of composites based on the unified macro- and micro-mechanics constitutive model. The relationship between stress and strain of both macro and micro composite structures can be calculated by the multi-scale finite element method and the unified macro- and micro-mechanics constitutive model. Then the micro-stress distribution was introduced into the failure criteria of the composite component to find out the danger point in the representative volume element and obtain the failure mode of it. In this paper, a new approach based on the unified macro- and micro-mechanics model is developed to analyze the failure of composite.

2. FVDAM

The unit cell representative of the material's microstructure was divided into rectangular sub-volumes and the displacement field in each sub-volume is expressed in terms of local coordinates. According to stress and displacement boundary condition of cell, the relationship between macro and micro quantities can be established. The stress and strain distribution in the unit cell can be analyzed by the micro-mechanics, if the macro-stress and displacement are given. Then the relationship between macro stress and strain of composite can be gained by homogenization in the unit cell.[7]

The microstructure of a multiphase composite is periodically distributed. The global coordinates (x_2, x_3) are defined such that the unit cell representative of the material microstructure is used to construct the periodic array, as illustrated in Fig. 1. Then the unit cell is discretized into $N_\beta \times N_\gamma$ sub-volumes, as illustrated in Fig. 2. The sub-volume (β,γ)'s local coordinate is $(\bar{y}_2^{(\beta)}, \bar{y}_3^{(\gamma)})$ and the origin of local coordinates is the geometric center point of sub-volume (β,γ), as illustrated

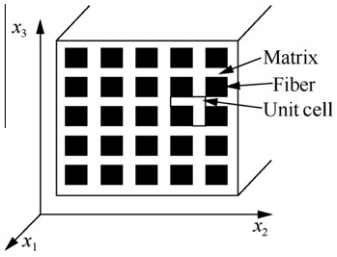

Fig. 1 Periodic microstructure of multiphase material.

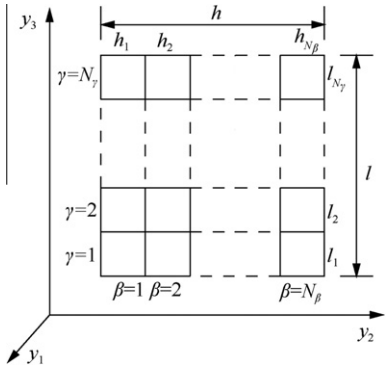

Fig. 2 A unit cell containing $N_\beta \times N_\gamma$ cells.

in Fig. 3. The displacement approximation in sub-volume (β,γ) has the form of

$$\begin{aligned} \boldsymbol{u}_i^{(\beta,\gamma)} &= \bar{\boldsymbol{\varepsilon}}_{ij} x_j + \boldsymbol{W}_{i(00)}^{(\beta,\gamma)} + \bar{y}_2^{(\beta)} \boldsymbol{W}_{i(10)}^{(\beta,\gamma)} + \bar{y}_3^{(\gamma)} \boldsymbol{W}_{i(01)}^{(\beta,\gamma)} \\ &\quad + \frac{1}{2}\left(3\left(\bar{y}_2^{(\beta)}\right)^2 - \frac{h_\beta^2}{4}\right) \boldsymbol{W}_{i(20)}^{(\beta,\gamma)} \\ &\quad + \frac{1}{2}\left(3\left(\bar{y}_3^{(\gamma)}\right)^2 - \frac{l_\gamma^2}{4}\right) \times \boldsymbol{W}_{i(02)}^{(\beta,\gamma)} \quad (i = 1,2,3) \end{aligned} \tag{1}$$

where $\bar{\varepsilon}_{ij} x_j$ denotes average displacements, $\boldsymbol{W}_{i(00)}^{(\beta,\gamma)}$ represents the fluctuating volume-averaged displacements, and $\boldsymbol{W}_{i(mn)}^{(\beta,\gamma)} (m,n = 0,1,2)$ the higher-order terms; h_β and l_γ are sizes of cell (β, γ) in the directions of $\bar{y}_2$ and $\bar{y}_3$ respectively, and the ranges of the indices β and γ are $\beta = 1, 2, \cdots, N_\beta$ and $\gamma = 1, 2, \cdots, N_\gamma$.

The displacement approximation of sub-volumes (β,γ) has another form:

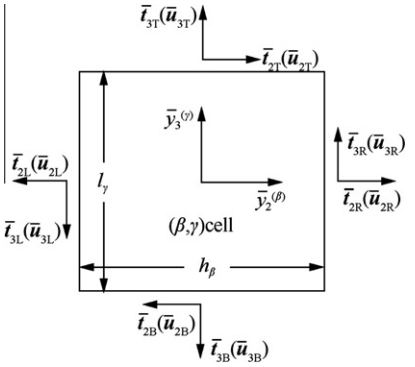

Fig. 3 Schematic of two-dimensional surface average displacement and stress.

$$\boldsymbol{u}_i^{(\beta,\gamma)} = \bar{\boldsymbol{\varepsilon}}_{ij} x_j + \tilde{\boldsymbol{u}}_i^{(\beta,\gamma)} \tag{2}$$

where $\tilde{\boldsymbol{u}}_i^{(\beta,\gamma)}$ variable displacements.

The average displacement on the left boundary of sub-volume (β,γ) is

$$\bar{\boldsymbol{u}}_{i\mathrm{L}}^{(\beta,\gamma)} = \frac{1}{l_\gamma}\int_{-l_\gamma/2}^{l_\gamma/2} \tilde{\boldsymbol{u}}_i^{(\beta,\gamma)}\left(-\frac{h_\beta}{2}, \bar{y}_3^{(\gamma)}\right)\mathrm{d}\bar{y}_3^{(\gamma)} \tag{3a}$$

The average displacement on the right, top and bottom boundaries of sub-volume (β,γ) are

$$\begin{cases} \bar{\boldsymbol{u}}_{i\mathrm{R}}^{(\beta,\gamma)} = \dfrac{1}{l_\gamma}\displaystyle\int_{-l_\gamma/2}^{l_\gamma/2} \tilde{\boldsymbol{u}}_i^{(\beta,\gamma)}\left(\frac{h_\beta}{2}, \bar{y}_3^{(\gamma)}\right)\mathrm{d}\bar{y}_3^{(\gamma)} \\ \bar{\boldsymbol{u}}_{i\mathrm{B}}^{(\beta,\gamma)} = \dfrac{1}{h_\beta}\displaystyle\int_{-h_\beta/2}^{h_\beta/2} \tilde{\boldsymbol{u}}_i^{(\beta,\gamma)}\left(\bar{y}_2^{(\beta)}, -\frac{l_\gamma}{2}\right)\mathrm{d}\bar{y}_2^{(\beta)} \\ \bar{\boldsymbol{u}}_{i\mathrm{T}}^{(\beta,\gamma)} = \dfrac{1}{h_\beta}\displaystyle\int_{-h_\beta/2}^{h_\beta/2} \tilde{\boldsymbol{u}}_i^{(\beta,\gamma)}\left(\bar{y}_2^{(\beta)}, \frac{l_\gamma}{2}\right)\mathrm{d}\bar{y}_2^{(\beta)} \end{cases} \tag{3b}$$

Substituting Eq. (1) into geometric equation (strain-displacement relationship), the strain in sub-volume (β,γ) is

$$\boldsymbol{\varepsilon}_{ij}^{(\beta,\gamma)} = \bar{\boldsymbol{\varepsilon}}_{ij} + \frac{1}{2}\left(\partial_i \tilde{\boldsymbol{u}}_j^{(\beta,\gamma)} + \partial_j \tilde{\boldsymbol{u}}_i^{(\beta,\gamma)}\right) \tag{4}$$

where $\partial_1 = 0$, $\partial_2 = \partial/\partial\bar{y}_2^{\beta}$ and $\partial_3 = \partial/\partial\bar{y}_3^{\gamma}$.

The non-zero strain components of sub-volume (β,γ) are given as follows:

$$\begin{cases} \boldsymbol{\varepsilon}_{11}^{(\beta,\gamma)} = \bar{\boldsymbol{\varepsilon}}_{11} \\ \boldsymbol{\varepsilon}_{22}^{(\beta,\gamma)} = \bar{\boldsymbol{\varepsilon}}_{22} + \boldsymbol{W}_{2(10)}^{(\beta,\gamma)} + 3\bar{y}_2^{(\beta)}\boldsymbol{W}_{2(20)}^{(\beta,\gamma)} \\ \boldsymbol{\varepsilon}_{33}^{(\beta,\gamma)} = \bar{\boldsymbol{\varepsilon}}_{33} + \boldsymbol{W}_{3(01)}^{(\beta,\gamma)} + 3\bar{y}_3^{(\gamma)}\boldsymbol{W}_{3(02)}^{(\beta,\gamma)} \\ \boldsymbol{\varepsilon}_{12}^{(\beta,\gamma)} = \bar{\boldsymbol{\varepsilon}}_{12} + \dfrac{1}{2}\left(\boldsymbol{W}_{1(10)}^{(\beta,\gamma)} + 3\bar{y}_2^{(\beta)}\boldsymbol{W}_{1(20)}^{(\beta,\gamma)}\right) \\ \boldsymbol{\varepsilon}_{13}^{(\beta,\gamma)} = \bar{\boldsymbol{\varepsilon}}_{13} + \dfrac{1}{2}\left(\boldsymbol{W}_{1(01)}^{(\beta,\gamma)} + 3\bar{y}_3^{(\gamma)}\boldsymbol{W}_{1(02)}^{(\beta,\gamma)}\right) \\ \boldsymbol{\varepsilon}_{23}^{(\beta,\gamma)} = \bar{\boldsymbol{\varepsilon}}_{23} + \dfrac{1}{2}\left(\boldsymbol{W}_{2(01)}^{(\beta,\gamma)} + \boldsymbol{W}_{3(10)}^{(\beta,\gamma)}\right) + \dfrac{3}{2}\left(\bar{y}_2^{(\beta)}\boldsymbol{W}_{3(20)}^{(\beta,\gamma)} + \bar{y}_2^{(\gamma)}\boldsymbol{W}_{2(02)}^{(\beta,\gamma)}\right) \end{cases} \tag{5}$$

The constitutive equation of sub-volume (β,γ) is

$$\boldsymbol{\varepsilon}^{(\beta,\gamma)} = \boldsymbol{S}^{(\beta,\gamma)}\boldsymbol{\sigma}^{(\beta,\gamma)} + \bar{\boldsymbol{\varepsilon}}^{\mathrm{p}(\beta,\gamma)} \tag{6}$$

where $\boldsymbol{S}^{(\beta,\gamma)}$ is compliance matrix and $\bar{\boldsymbol{\varepsilon}}^{\mathrm{p}(\beta,\gamma)}$ inelastic strain.

For elastic materials, Hook's law is expressed as:

$$\boldsymbol{\sigma}_{ij} = \boldsymbol{C}_{ijkl}\boldsymbol{\varepsilon}_{kl} \tag{7}$$

where $\boldsymbol{C}_{ijkl}$ denotes stiffness matrix of the elements.

The force of unit area is

$$\boldsymbol{t}_i^n = \boldsymbol{\sigma}_{ij}\boldsymbol{n}_j \tag{8}$$

where $\boldsymbol{n}_j$ donates the cosine of the outside normal direction.

Integrating Eq. (8) into the sub-volume's boundary conditions, all average stress components are given on the boundary. The average stresses on left, right, bottom and top boundary the sub-volume (β,γ) are

$$\begin{cases} \bar{\boldsymbol{\sigma}}_{i\mathrm{L}}^{(\beta,\gamma)} = \dfrac{1}{l_\gamma}\displaystyle\int_{-l_\gamma/2}^{l_\gamma/2} \boldsymbol{t}_i^{n(\beta,\gamma)}\left(-\frac{h_\beta}{2}, \bar{y}_3^{(\gamma)}\right)\mathrm{d}\bar{y}_3^{(\gamma)} \\ \bar{\boldsymbol{\sigma}}_{i\mathrm{R}}^{(\beta,\gamma)} = \dfrac{1}{l_\gamma}\displaystyle\int_{-l_\gamma/2}^{l_\gamma/2} \boldsymbol{t}_i^{n(\beta,\gamma)}\left(\frac{h_\beta}{2}, \bar{y}_3^{(\gamma)}\right)\mathrm{d}\bar{y}_3^{(\gamma)} \\ \bar{\boldsymbol{\sigma}}_{i\mathrm{B}}^{(\beta,\gamma)} = \dfrac{1}{h_\beta}\displaystyle\int_{-h_\beta/2}^{h_\beta/2} \boldsymbol{t}_i^{n(\beta,\gamma)}\left(\bar{y}_2^{(\beta)}, -\frac{l_\gamma}{2}\right)\mathrm{d}\bar{y}_2^{(\beta)} \\ \bar{\boldsymbol{\sigma}}_{i\mathrm{T}}^{(\beta,\gamma)} = \dfrac{1}{h_\beta}\displaystyle\int_{-h_\beta/2}^{h_\beta/2} \boldsymbol{t}_i^{n(\beta,\gamma)}\left(\bar{y}_2^{(\beta)}, \frac{l_\gamma}{2}\right)\mathrm{d}\bar{y}_2^{(\beta)} \end{cases} \tag{9}$$

The displacements on the boundary of two neighboring sub-volumes at the average value are continuous:

$$\begin{cases} \bar{\boldsymbol{u}}_{i\mathrm{R}}^{(\beta,\gamma)} = \bar{\boldsymbol{u}}_{i\mathrm{L}}^{(\beta+1,\gamma)} \\ \bar{\boldsymbol{u}}_{i\mathrm{T}}^{(\beta,\gamma)} = \bar{\boldsymbol{u}}_{i\mathrm{B}}^{(\beta,\gamma+1)} \end{cases} \tag{10}$$

Periodic displacement boundary conditions of the unit cell are

$$\begin{cases} \bar{\boldsymbol{u}}_{i\mathrm{R}}^{(N_\beta,\gamma)} = \bar{\boldsymbol{u}}_{i\mathrm{L}}^{(1,\gamma)} \\ \bar{\boldsymbol{u}}_{i\mathrm{T}}^{(\beta,N_\gamma)} = \bar{\boldsymbol{u}}_{i\mathrm{B}}^{(\beta,1)} \end{cases} \tag{11}$$

The relationships between two neighboring sub-volumes at the boundary are

$$\begin{cases} \bar{\boldsymbol{\sigma}}_{i\mathrm{R}}^{(\beta,\gamma)} + \bar{\boldsymbol{\sigma}}_{i\mathrm{L}}^{(\beta+1,\gamma)} = \boldsymbol{0} \\ \bar{\boldsymbol{\sigma}}_{i\mathrm{T}}^{(\beta,\gamma)} + \bar{\boldsymbol{\sigma}}_{i\mathrm{B}}^{(\beta,\gamma+1)} = \boldsymbol{0} \end{cases} \tag{12}$$

And the periodic stress boundary conditions of the unit cell are

$$\begin{cases} \bar{\boldsymbol{\sigma}}_{i\mathrm{L}}^{(1,\gamma)} + \bar{\boldsymbol{\sigma}}_{i\mathrm{R}}^{(N_\beta,\gamma)} = \boldsymbol{0} \\ \bar{\boldsymbol{\sigma}}_{i\mathrm{B}}^{(\beta,1)} + \bar{\boldsymbol{\sigma}}_{i\mathrm{T}}^{(\beta,N_\gamma)} = \boldsymbol{0} \end{cases} \tag{13}$$

When the structure is in equilibrium, the micro stress distributing must satisfy the equilibrium equation:

$$\frac{1}{A_{(\beta,\gamma)}}\int_{-h_\beta/2}^{h_\beta/2}\int_{-l_\gamma/2}^{l_\gamma/2} \boldsymbol{\sigma}_{ji,j}^{(\beta,\gamma)}\mathrm{d}\bar{y}_2^{(\beta)}\mathrm{d}\bar{y}_3^{(\gamma)} = \boldsymbol{0} \tag{14}$$

where $A_{(\beta,\gamma)}$ is the area of the sub-volume.

Totaling Eq. (14) in the unit cell, the macro-stress which is the average stress of the unit cell is

$$\bar{\boldsymbol{\sigma}} = \frac{1}{hl}\sum_{\beta=1}^{N_\beta}\sum_{\gamma=1}^{N_\gamma} h_\beta l_\gamma \bar{\boldsymbol{\sigma}}^{(\beta,\gamma)} \tag{15}$$

The macro constitutive equation of composite is

$$\bar{\boldsymbol{\sigma}} = \boldsymbol{C}^*\bar{\boldsymbol{\varepsilon}} \tag{16}$$

Solving Eq. (16), the stiffness matrix $\boldsymbol{C}^*$ is obtained.

Using Eq. (2) and Eqs. (9)–(13), the relationship between the macro strain and the average displacement on the cell's boundary can be obtained.[6–8] If the macro stress distribution is known, the macro strain with the macro constitutive equation of composite and the average displacement on every sub-volume's boundary can be given. Then, solving Eq. (2), the higher-order displacement terms $\boldsymbol{W}_{i(mn)}^{(\beta,\gamma)}$ of the sub-volume (β, γ) are also given. Finally, the micro stress and strain distributing can be solved in the sub-volume (β, γ) with Eqs. (5) and (6).

3. Unified Macro- and micro-mechanical failure criteria of composite based on FVDAM

In this paper, a progressive failure analytical model based on the unified macro- and micro-mechanical method is proposed. Similar to other progressive failure analytical methods, this method is made up of three major parts, the stress analysis, the failure analysis as well as the degeneration of the properties of the materials. This analytical model involves the combination of the macro and micro analysis, thus, analytical flow of it is much more complex than that of the traditional macro progressive failure analysis. The basic steps of the analysis are shown in Fig. 4.

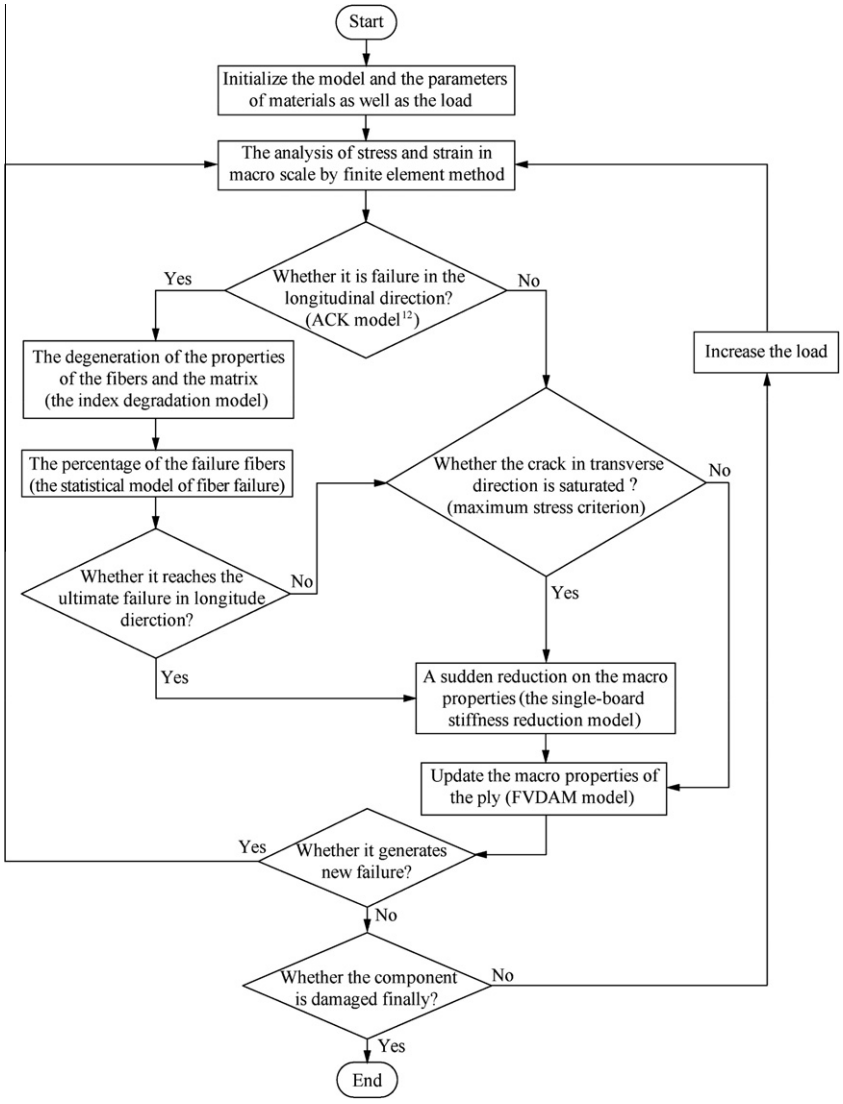

Fig. 4 Flowchart of progressive failure analytical model based on unified macro- and micro-mechanical method.

4. Damage analysis of composite structure

The unified macro- and micro-failure criteria were used for analyzing the damage of a composite plate with a hole and the results were compared with those of macro failure criteria.

4.1. Stress analysis of composite structure

The dimensions of the composite plate were 200 mm and 100 mm along x and y axes respectively, and thickness of plate was 3 mm. The radius of circular hole in the center of plate was 40 mm (see Fig. 5). The direction of fibers was along x axis and the fiber volume fraction was 0.62. The left surface of plate was fixed. There were two kinds of load on the right surface. The pressure P_A which valued 100 MPa was along x axis and the concentrated force P_B was 3 kN. Point A was on the edge of the hole and θ was the angle clockwise rotated from y axis to line O'^A. The composite plate was assumed transversely isotropic. Therefore, only four independent elastic constants were required for two-dimensional (plane stress) analysis. The mechanical properties of fiber and matrix are given in Table 1, and the results of macro-mechanical performance of unidirectional laminate are also given.

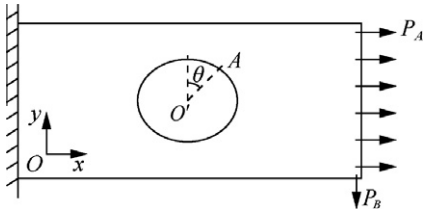

Fig. 5 Composite component with hole subject to uniform pressure or concentrated load.

The macro stress distribution of composite plate can be calculated with finite element method (see Fig. 6). Because the location of maximum stress is on the edge of the hole at

Table 1 Material constant of fiber or matrix or composite.

Material constant	E-glass21K43 Gevetex fiber[13]	LY556/HT907/DY063 epoxy matrix[13]	Unidirectional laminate	
Longitudinal modulus E_1(GPa)	80	3.35	53.48[a]	50.904[b]
Transverse modulus E_2(GPa)	80	3.35	17.7[a]	16.755[b]
In-plane shear modulus G_{12}(GPa)	33.33	1.24	5.83[a]	5.093[b]
Through thickness Poisson's ratio μ_{23}	0.2	0.35	0.4[a]	0.24[b]
Longitudinal tensile strength X_t(MPa)	1804.1[14]	56.5[14]	1140[a]	
Longitudinal compressive strength X_c(MPa)	908.9[14]	55.7[14]	570[a]	
Transverse tensile strength Y_t(MPa)			35[a]	
Transverse compressive strength Y_c(MPa)			114[a]	
In-plane shear strength S_{12}(MPa)			72[a]	

[a] Experimental value.[12]
[b] The results of FVDAM.

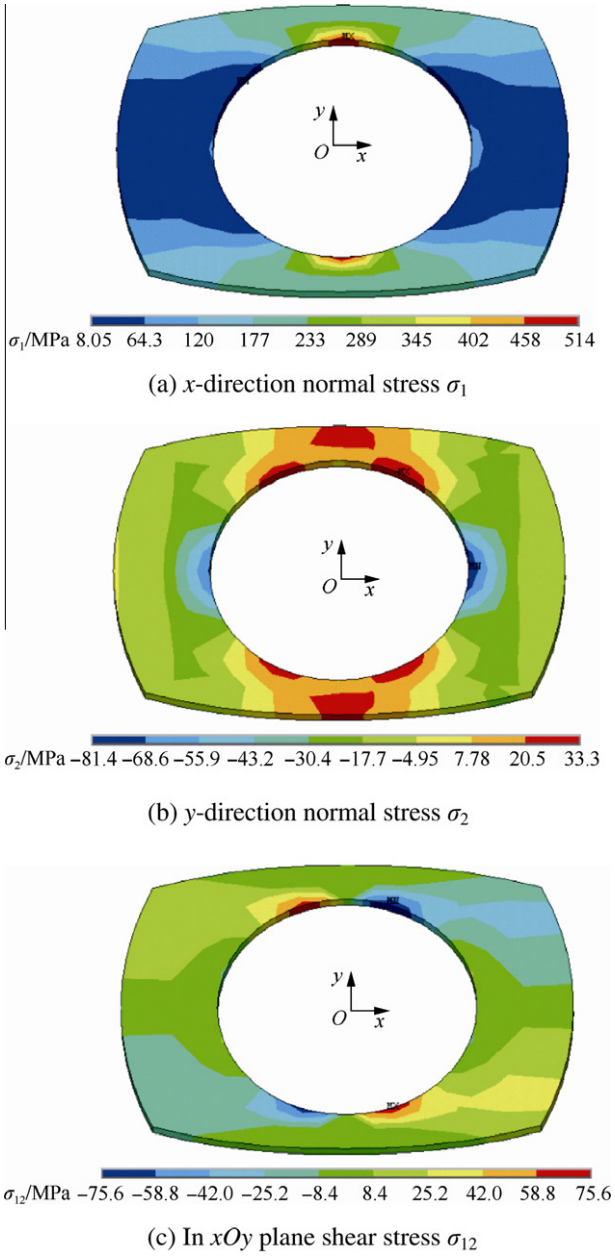

(a) x-direction normal stress σ_1

(b) y-direction normal stress σ_2

(c) In xOy plane shear stress σ_{12}

Fig. 6 Stress distribution of hole's side at P_A load.

the contribution of P_A or P_B, it is the primary region of interest.

4.2. Damage analysis with the macro failure criteria

The maximum stress criteria and Hashin criteria were adopted, which are called Criteria 1 and Criteria 2 for short. Both Criteria 1 and Criteria 2 considered that there were three damage modes of composite: fiber fracture, matrix cracking and matrix-fiber shear failure (see Table 2). Criteria 1 and Criteria 2 were used for judging damage modes of composite around the hole.

When only P_A was applied, the relationship curves between the stress components σ_1 and θ on the hole's edge was mapped (see Fig. 7). The strength of unidirectional laminate was also given in Fig. 7. According to Criteria 1, the fiber fracture could not occur. And results of two other damage modes are shown in Figs. 8 and 9 (in Fig. 9, S_p and S_n denote the interfacial shear stress during tension and push process) respectively. The matrix-fiber shear failure occurred at $\theta = 20°$ and $\theta = 160°$ with Criteria 1. In the same way matrix cracking and matrix-fiber shear failed at $\theta = 20°$,160°,200°,340° with Criteria 2. When only P_B was applied, the results with Criteria 1 were in accordance with ones with Criteria 1 and matrix cracking occurred at $\theta = 50°$ and $\theta = 230°$.

4.3. Damage analysis with unified macro- and micro-failure criteria

Macro-stress distribution in structure and micro-stress in the unit cell were calculated with corresponding method. The damage forms of composite were estimated by the stress components of fiber and matrix. And the macro-stress distribution of dangerous point would be calculated in prior.

4.3.1. Failure point

According to the results of Criteria 1 and Criteria 2, the damage points of composite plate were at $\theta = 20°$ and $\theta = 160°$ if P_A was applied only, and they were at $\theta = 50°$ and $\theta = 230°$ for P_B. Therefore, they were considered as failure points and micro-stress distribution in the unit cell of these points would be calculated.

Table 2 The proposed macro-mechanical failure criteria of composite.

Damage mode	Maximum stress criterion	Hashin criteria[15]
Fiber fracture	$\begin{cases}\sigma_1/X_t=1,\ \sigma_1>0\\ \sigma_1/X_c=1,\ \sigma_1\leqslant 0\end{cases}$	$\begin{cases}(\sigma_1/X_t)^2=1,\sigma_1>0\\ (\sigma_1/X_c)^2=1,\sigma_1\leqslant 0\end{cases}$
Matrix cracking	$\begin{cases}\sigma_2/Y_t=1,\ \sigma_2>0\\ \sigma_2/Y_c=1,\ \sigma_2\leqslant 0\end{cases}$	$\begin{cases}(\sigma_2/Y_t)^2+(\tau_{12}/S_{12})^2=1,\ \sigma_2>0\\ (\sigma_2/Y_c)^2+(\tau_{12}/S_{12})^2=1,\ \sigma_2\leqslant 0\end{cases}$
Matrix-fiber shear	$\tau_{12}/S=1$	$\begin{cases}(\sigma_1/X_t)^2+(\tau_{12}/S_{12})^2=1,\ \sigma_1>0\\ (\sigma_1/X_c)^2+(\tau_{12}/S_{12})^2=1,\ \sigma_1\leqslant 0\end{cases}$

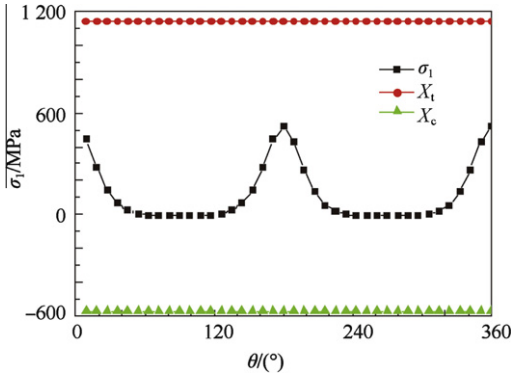

Fig. 7 Fiber break estimated by maximum stress criterion at P_A load.

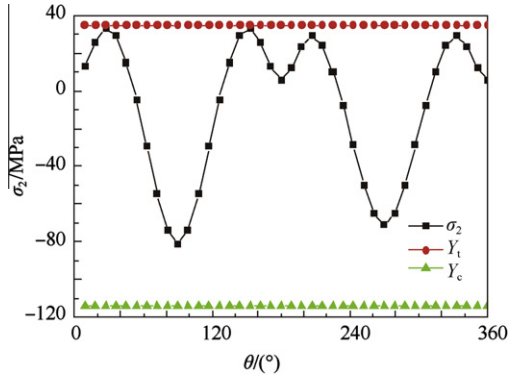

Fig. 8 Matrix crack estimated by maximum stress criterion at P_A load.

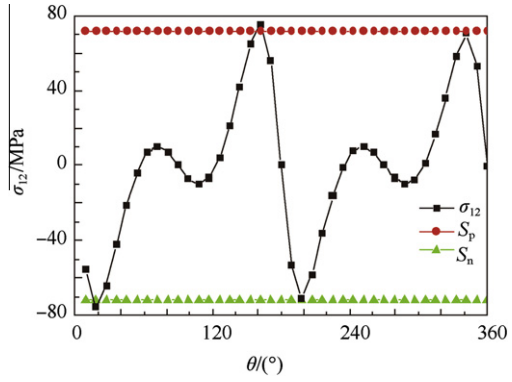

Fig. 9 Interfacial shear estimated by maximum stress criterion at P_A load.

4.3.2. Damage analysis based on micro stress field

When P_A or P_B was applied, micro-stress distribution of failure points is shown in Figs. 10 and 11. The failed cells in the unit cell were judged by the comparison of experimental values of fiber and matrix strength.

In Fig. 10, the equivalent stress of matrix at neighborhood of interface, left and right parts of the unit cell exceeded the matrix strength X_t and X_c, so matrix cracking and interface failure occurred, which had good coincidence with Hashin criteria. In Fig. 11, the equivalent stress of matrix at left and right parts of the unit cell exceeded X_t and X_c, matrix cracking occurred and the resolution was similar to macro failure criteria.

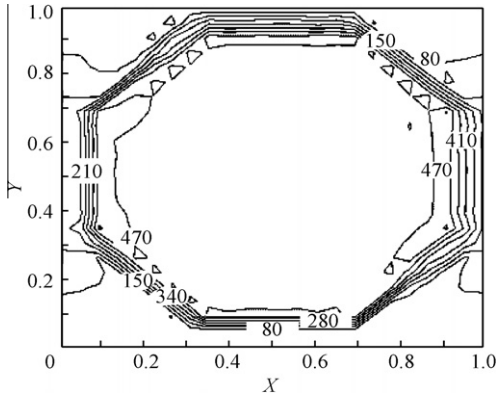

Fig. 10 Unit cell σ_{eqv} (MPa) distribution of dangerous point at P_A load.

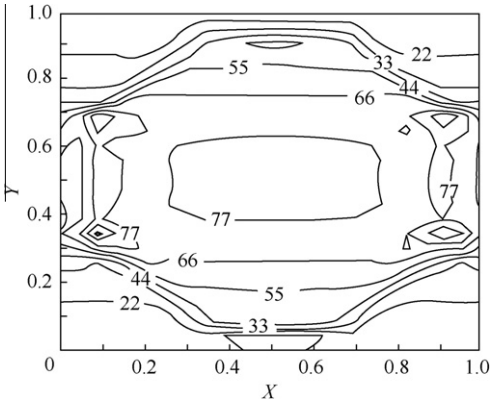

Fig. 11 Unit cell σ_{eqv} (MPa) distribution of dangerous point at P_B load.

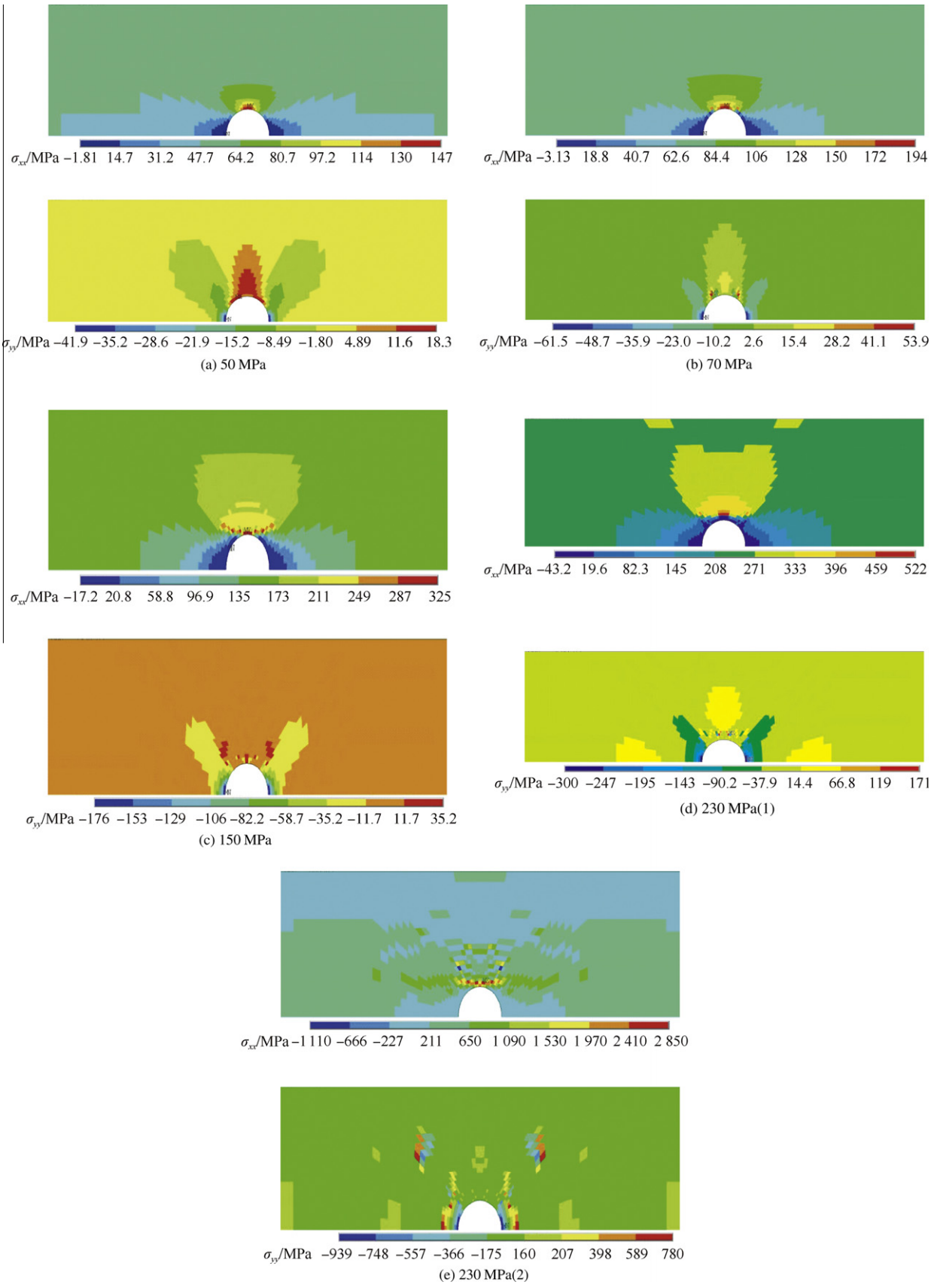

Fig. 12 Failure progress of unidirectional composite plate with a center hole.

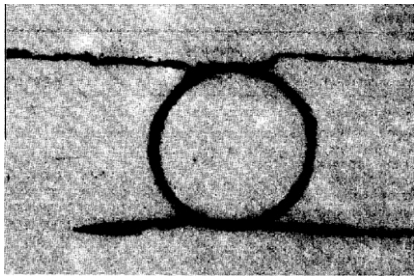

Fig. 13 Photo of the crack around the hole.

4.4. Progressive failure analysis of unidirectional composite plate with a hole

In this article, the progressive failure analytical model based on the unified macro- and micro-mechanical method was used to simulate the failure progress of the unidirectional composite plate with a center hole in it. A series of stress distribution around the hole at different P_A load levels is shown in Fig. 12(a–e).

As shown in Fig. 12, at a lower load (50 MPa), every point in the component did not fail, but there was significant stress concentration around the hole. When the load was 70 MPa, the cracking in the transverse direction occurred at the point with an angle about 60° with x-axis around the edge of the hole for the first time, which would lead to the redistribution of the stress. With the increase of load, the cracking developed along the x-axis. When the load was 230 Mpa (Fig. 12(d–e)), the failure of the fibers firstly occurred at the point with an angle about 90° with x-axis, as illustrated in Fig. 12(d), which will result in the re-distribution of stress, then kept the load at 230 MPa; the fibers of a series of elements failed, through iterative calculation, we can obtain the ultimate distribution of stress at 230 MPa, as illustrated in Fig. 12(e), which means the failure of the component. Thus, the failure load of the component was 230 MPa.

Fig. 13 gives the photo of the crack around the hole in the unidirectional SiC/1732 composite plate with a center hole under uniaxial tensile load.[16] SiC/1732 is a kind of SiC fibers reinforce glass matrix composites, which has similar mechanical properties to that of the SiC/CAS composites. In Fig. 13, it can be found that transverse cracking failure in the SiC/1732 composite plate with a center hole firstly occurred at the edge of the hole with an angle of nearly 60° between the x-axis, then would develop along the longitudinal direction similar to the simulation in this paper. Thus, the progressive failure analytical model based on the unified macro- and micro-mechanical method proposed in this paper can be applied to the progressive failure analysis of ceramic matrix composites.

5. Conclusions

A unified macro- and micro-mechanics strength model is developed, which is a multi-scale finite element method based on FVDAM. In composite structure, macro-stress distribution can be calculated by FEM with boundary condition, and FVDAM is used for computing micro-stress in the unit cell. The micro stress distribution on the damage location will be compared with the strength of fiber or matrix to estimate the failure mode. The developed method is used to analyze a composite plate with a circular hole and the results are in accordance with the ones of macro failure criteria. It proves the validity and effectiveness of the unified macro- and micro-mechanical damage analysis method.

Acknowledgement

This study was co-supported by National Basic Research Program of China, National Natural Science Foundation of China (No. 51075204), Aeronautical Science Foundation of China (No. 2009ZB52028, No. 2012ZB52026), Research Fund for the Doctoral Program of Higher Education of China (No. 20070287039), and NUAA Research Funding (No. NZ2012106)

References

1. Lei C. Macro- and micro-mechanics strength analysis of composite structures. dissertation. Nanjing: Nanjing University of Aeronautics and Astronautics; 2006 [Chinese].
2. Aboudi J. Micromechanical analysis of composites by method of cells. *Appl Mech Rev* 1989;**42**(7):193–221.
3. Paley M, Aboudi J. Micromechanical analysis of composites by the generalized cells method. *Mech Mater* 1992;**14**(2):127–39.
4. Pindera MJ, Bednarcyk BA. An efficient implementation of the generalized method of cells for unidirectional, multi-phased composites with complex microstructures. *Compos Part B*. 1999;**30**(2):87–105.
5. Aboudi J, Pindera MJ, Arnold SM. High-fidelity generalized method of cells for inelastic periodic multiphase materials; 2002. Report No.: NASA TM 2002–211469.
6. Bansal Y, Pindera M. A second look at the higher-order theory for periodic multiphase materials. *J Appl Mech* 2005;**72**(2):177–95.
7. Bansal Y, Pindera M. Finite-volume direct averaging micromechanics of heterogeneous materials with elastic-plastic phases. *Int J Plasticity* 2006;**22**(5):775–825.
8. Khatam H, Pindera M. Parametric finite-volume micromechanics of periodic materials with elastoplastic phases. *Int J Plasticity* 2009;**25**(7):1386–411.
9. Sun Z, Lee L, Zhu B. Effect of inter-face layer parameters on uniaxial tensile behavior of ceramic matrix composites. *J Aerosp Power* 2010;**25**(3):597–602 [Chinese].
10. Sun Z, Song Y, Gao D. Efficient reformulation of 2-D high-fidelity generalized method of cells. *Acta Mechanica Solida Sinica* 2005;**26**(2):235–40 [Chinese].
11. Sun Z, Gao X, Song Y. Efficient reformulation of 3-D high-fidelity generalized method of cells. *J Aerosp Power* 2008;**23**(7):1318–22 [Chinese].
12. Aveston J, Kelly A. Theory of multiple fracture on fibrous composites. *J Mater Sci* 1973;**8**(3):352–62.
13. Soden PD, Hinton MJ, Kaddour AS. Lamina properties, lay-up configurations and loading conditions for a range of fiber-reinforced composite laminates. *Comp Sci Technol* 1998;**58**(7):1011–22.
14. Huang Z. A bridging model prediction of the ultimate strength of composite laminates subjected to biaxial loads. *Comp Sci Technol* 2004;**64**(3):395–448.
15. Hashin Z. Failure criteria for unidirectional fiber composites. *J Appl Mech* 1980;**47**(2):329–34.
16. Mall S, Bullock DE, Pernot JJ. Tensile fracture behaviour of fiber-reinfored ceramic-matrix composite with hole. *Compos Part A Appl Sci Manuf* 1993;**25**(3):237–42.

Sun Zhigang received the B.S. degree in aerospace propulsion theory and engineering from Nanjing University of Aeronautics and Astronautics in 2005 and then became a teacher there. His main research interests are the mechanical properties and structure design of ceramic matrix composite.